Effect of the Conformational Kinetic Energy and the Rotovibrational Coupling in the Conformational Population of Bioactive Compounds

A. Niño,* C. Muñoz-Caro, M. Mora, and S. Reyes

Grupo de Química Computacional, E. S. Informática, Universidad de Castilla-La Mancha, Paseo de la Universidad 4, 13071, Ciudad Real (Spain)

Received: August 21, 2003; In Final Form: October 2, 2003

This work presents the determination of a semiclassical conformational partition function for bioactive compounds. The proposed partition function includes the effect of the rotovibrational coupling and the conformational kinetic energy, through the rotovibrational G matrix. In addition, the model considers a relaxed potential that includes the effect of the nonconformational, internal, coordinates. Comparison of results from harmonic and anharmonic vibrational models shows that the present partition function is a good approximation to the quantum one. The effect of the rotovibrational coupling and conformational kinetic energy, i.e. the G matrix, on the partition function is analyzed considering the biologically active, protonated, forms of nicotine and the nicotinic analgesic ABT-594. All energetic and structural data are derived from ab initio results at the MP2/cc-pVDZ level. Only two conformers are found to be significantly populated at physiological temperature in the nicotine case. The relative population of both conformers is clearly affected by the value of the G matrix. For ABT-594, several minima on the conformational potential energy hypersurface are found. However, only one conformer collects the population. Here, the distribution of population is only slightly affected by the G matrix. Performing simulations with a double minima potential, we show that for conformers separated by energy differences about or higher than 2 kcal mol^{-1}, the effect of the G matrix can be neglected.

Introduction

Conformational flexibility is an important factor to take into account when modeling the activity of bioactive compounds. In particular, the three-dimensional arrangement of pharmacophoric groups is a function of the conformational coordinates. To adopt the optimal disposition for interaction with the receptor's active site, the conformational coordinates of the bioactive agent must change accordingly.

Usually, the conformational problem is tackled from a conformational analysis on the considered coordinates. Thus, on the grounds of the Born−Oppenheimer approximation, we obtain a potential energy hypersurface for the conformational motion. Minima on this hypersurface (and specially the global minimum) are considered as candidates for the optimal pharmacophore distribution. However, this information lacks the entropic effects. On the other hand, when interacting with the receptor site, the conformation of interest is the one corresponding to a minimum of Gibbs energy for the ligand-active site complex. Therefore, two conclusions can be drawn. First, rather than using energetic criteria, a thermostatistical point of view is needed. Second, to account for the possible variation of conformation when interacting with the receptor, the set of conformations accessible for a given interaction energy must be considered. From this point of view, the key point is the evaluation of a conformational partition function.

The conformational partition function for bioactive compounds is usually obtained from a Boltzmann distribution involving only the conformational potential energy.[1−3] This technique is rooted on a series of works related to the determination of the semiclassical conformational partition function in macromolecules.[4−7] From the physical standpoint, the exclusive use of the conformational potential energy implies two assumptions. First, the inertial moments remain unchanged over all the conformational space. Second, the conformational kinetic energy is also constant. Strictly speaking, these two assumptions are unjustified for a typical bioactive compound where the conformational variation is translated in the motion of large moieties within the molecule.

The computation of a conformational partition function using approximate molecular models was considered by Gõ and Scheraga in ref 7. These authors consider two models. The first one is the "classical flexible model". In this case, the conformational potential energy is defined by the minimum potential energy for fixed (time-averaged) values of the conformational coordinates. The kinetic energy is handled in Cartesian coordinates. In the semiclassical partition function, the integration of the momenta (kinetic part) gives a constant term. Integration of the coordinates (potential part) is carried out in internal coordinates. However, in this last integration, both the Jacobian of the Cartesian to internal coordinates transformation and the force constants for the nonconformational coordinates are considered constant. The result depends only on the conformational potential energy. The second model considered in ref 7 is the "classical rigid model". Here, the potential depends only on the conformational coordinates for fixed values of the remaining internal coordinates. The semiclassical partition function is obtained using internal coordinates, excluding the nonconformational coordinates and the overall rotation. Integration of momenta yields a matrix of kinetic terms depending on the conformational coordinates. Now, the partition function involves both the conformational kinetic energy matrix and the conformational potential energy. The detailed comparison presented in ref 7 shows that both models are approximate, with

* Corresponding author. E-mail: quimcom@uclm.es, Tel.: (+34)-926295362, Fax: (+34)926295354.

10.1021/jp036486y CCC: $25.00
Published on Web 11/11/2003

the first (the flexible model) being more realistic and accurate than the second (the rigid model).

The problem of the construction of a less approximate molecular model for conformational motions can be tackled from the standpoint of the theoretical study of large amplitude vibrations. These vibrations are responsible for the conformational flexibility. The classical example of such vibrations is the torsional motion (internal rotation) of methyl groups. These studies begin by solving the vibrational Schrödinger equation for the anharmonic, large amplitude variation of internal coordinates.[8] Today ab initio methodology is used, and the potential energy for the considered motion is obtained by relaxing the molecular geometry for fixed values of the large amplitude (conformational) coordinates.[9] In turn, the kinetic energy terms are obtained from the elements of the rotovibrational G matrix,[10] considering the overall rotation and the conformational coordinates. These kinetic terms are derived from the relaxed molecular structures.[9] In this form, the vibrational energy levels are computed. The results show that the theoretical vibrational energy levels differ from the experimentally observed levels by a few wavenumbers, see for instance refs 9c and 9d. These studies indicate that the effect of the variation of the rotovibrational coupling and the conformational kinetic energy is relevant. From the point of view of the potential, the data show that the potentials obtained by relaxing the molecular geometries for fixed values of the conformational coordinates actually represent the potential for the conformational motion. These potentials are formally very close, but not identical, to the potential used in the "classic flexible model" for the computation of the partition function.[7] In addition, the reliability of the results depends mainly on the quality of the potential energy function, see for instance ref 11.

In this work, we revisit the calculation of a conformational partition function for molecular systems. We consider systems with the size of usual bioactive compounds, where ab initio methodology can be applied. Thus, we develop a semiclassical rotovibrational partition function for a molecule with several conformational degrees of freedom. The model considers the overall rotational and the conformational coordinates, with a fully relaxed potential for fixed conformational coordinates. No additional restrictions are introduced. Thus, the model includes the effect of the conformational kinetic energy and the rotovibrational coupling. In addition, we analyze the validity of the semiclassical partition function by comparison with results for harmonic and large amplitude vibrational models. Finally, the effect of the conformational kinetic energy and the rotovibrational coupling in the conformational populations of nicotine and the new nicotinic analgesic ABT-594 is presented.

Theoretical Treatment

We start by considering a molecule with m conformational degrees of freedom. Using internal coordinates, the semiclassical partition function for the rotovibrational motions, z_{rv}, is obtained as[12]

$$z_{rv} = h^{-(m+3)} \int_Q \int_P \exp[-H(P,Q)/kT] \prod_i^{m+3} dp_i\, dp_i \quad (1)$$

where $H(P,Q) = T(P) + V(Q)$ is the classical Hamiltonian defined in terms of conjugated pairs of momenta, P, and coordinates, Q, for the overall rotation and conformational motions. For N atoms, the kinetic energy, $T(P)$, can be obtained in velocity representation as[8,13]

$$T(V) = \frac{1}{2} \sum_\alpha^N m_\alpha \boldsymbol{V}_\alpha \cdot \boldsymbol{V}_\alpha \quad (2)$$

where

$$\boldsymbol{V}_\alpha = \boldsymbol{V} + (\omega \times \mathbf{r}_\alpha) + \sum_{i=6}^{3N} \frac{\partial \mathbf{r}_\alpha}{\partial q_i} \dot{q}_i \quad (3)$$

In eq 3, $\boldsymbol{V}$ represents the velocity of the center of mass, ω is the angular velocity, $\mathbf{r}_\alpha$ is the position vector of the α atom, and q_i are the internal coordinates. By using center of mass coordinates, matrix notation, and deriving $T(V)$ with respect to the velocities, we obtain the kinetic energy in terms of momenta[8]

$$T(P) = \frac{1}{2} \mathbf{P}^T \mathbf{G} \mathbf{P} \quad (4)$$

Here, $\mathbf{P}$ is the column matrix of momenta, $\mathbf{P}^T$ its transpose, and $\mathbf{G}$ is the rotovibrational matrix defined as

$$\mathbf{G} = \begin{bmatrix} \mathbf{I} & \mathbf{X} \\ \mathbf{X}^T & \mathbf{Y} \end{bmatrix}^{-1} \quad (5)$$

In eq 5, $\mathbf{I}$ represents the inertial tensor, i.e., the pure rotational contribution, $\mathbf{Y}$ corresponds to the pure vibrational contribution, and $\mathbf{X}$ is the rotation−vibration interaction (Coriolis term). The elements of these matrices are obtained from the molecular geometry as

$$I_{ij} = -\sum_\alpha^n m_\alpha \mathbf{r}_{\alpha i} \mathbf{r}_{\alpha j}$$

$$I_{ii} = \sum_\alpha^n m_\alpha [(\mathbf{r}_\alpha)^2 - \mathbf{r}_{\alpha i}^2]$$

$$X_{ij} = \sum_\alpha^n m_\alpha \left[\mathbf{r}_\alpha \times \frac{\partial \mathbf{r}_\alpha}{\partial q_i} \right]_j$$

$$Y_{ij} = \sum_\alpha^n m_\alpha \frac{\partial \mathbf{r}_\alpha}{\partial q_i} \cdot \frac{\partial \mathbf{r}_\alpha}{\partial q_j} \quad (6)$$

Using eq 4 and the potential energy, the quantum mechanical Hamiltonian for pure vibrations can be obtained by applying the Podolsky transformation.[14] The expression reads[8]

$$\hat{H} = -\sum_i^m \sum_j^m \left[B_{ij} \frac{\partial^2}{\partial q_i \partial q_j} + \left(\frac{\partial B_{ij}}{\partial q_i} \right) \frac{\partial}{\partial q_j} \right] + V(Q) \quad (7)$$

where the kinetic terms B_{ij} are defined as $B_{ij} = \hbar^2 g_{ij}/2$, with g_{ij} being the corresponding element of the G matrix. The potential $V(Q)$ is given in internal coordinates. Equation 7 will be applied afterward.

Equation 1 is defined in the framework of the Hamilton formulation of mechanics. Thus, we must work with holonomic systems,[15] in other words, with systems where the generalized coordinates are independent of each other. However, when using the ω angular velocity we have a constraint (constant ω) between the components of the velocity, but not between the coordinates. So, the constraint cannot be expressed as a relation between the coordinates in the form $f(\mathbf{r}_1, \mathbf{r}_2, .., \mathbf{r}_n) = 0$. This is another way of saying that the coordinates are nonholonomic.[15]

Therefore, eq 4 cannot be introduced directly in eq 1. To use eq 1 we must begin with a holonomic set of overall rotational coordinates, for instance, the usual Euler angles (θ, ϕ, ψ).[15] Thus, eq 1 becomes

$$z_{rv} = h^{-(m+3)} \int_Q \int_P \exp[-T_E(P)/kT] \times \exp[-V(Q)/kT]\, dP_\theta\, d\theta\, dP_\phi\, d\phi\, dP_\psi\, d\psi \prod_{i=4}^{m+3} dp_i\, dq_i \quad (8)$$

where T_E indicates that the kinetic energy is expressed in terms of Euler angles. Thus, eq 4 can be introduced in eq 8 using the principal axis as internal axis. In this form, it is possible to change the differential of Euler moments to a differential of angular moments using the Jacobian of the transformation:[15] $\sin(\theta)$. Integrating the Jacobian and substituting eq 4 in eq 8 we obtain

$$z_{rv} = 8\pi^2 h^{-(m+3)} \int_Q \int_P \exp[-\mathbf{P}^T\mathbf{G}\mathbf{P}/2kT] \prod_{i=1}^{m+3} dp_i \times \exp[-V(Q)/kT] \prod_{i=4}^{m+3} dq_i \quad (9)$$

In eq 9, the kinetic energy part, i.e., the G matrix, depends on the coordinates, and the coordinates considered are reduced to the conformational ones.

The kinetic energy term can be integrated by reducing the rotovibrational G matrix to a diagonal form, **D**, using an orthogonal transformation,

$$\mathbf{D} = \mathbf{W}^T\mathbf{G}\mathbf{W} \quad (10)$$

where **W** is the transformation matrix. The matrix **D** represents the kinetic matrix in a coordinate system where it is diagonal. Thus, the effect of the **D** matrix is to perform a rotation of coordinates from the principal axis system. The matrix of the transformation to the new momenta system is **W**. Since **W** is orthogonal, its determinant (Jacobian of the transformation) is unity. Therefore,

$$z_{rv} = 8\pi^2 h^{-(m+3)} \int_Q \prod_{i=1}^{m+3} [\int_P \exp[-d_{ii}/2kT]\, dp_i] \times \exp[-V(Q)/kT] \prod_{i=4}^{m+3} dq_i \quad (11)$$

where d_{ii} are the diagonal elements of the **D** matrix. Since

$$\int_{-\infty}^{+\infty} \exp(-ax^2)\, dx = (\pi/a)^{1/2} \quad (12)$$

we obtain,

$$z_{rv} = 8\pi^2 \left(\frac{2\pi kT}{h^2}\right)^{(m+3)/2} \int_Q |G(Q)|^{-1/2} \times \exp[-V(Q)/kT] \prod_{i=4}^{m+3} dq_i \quad (13)$$

where $|G(Q)|$ is the determinant of the G matrix. Equation 13 resembles the semiclassical rotovibrational partition function for the "classical rigid model" of ref 7. However, here the rotovibrational coupling is included in the G matrix. The model is fully flexible, since all the internal coordinates are allowed to vary when obtaining the potential.

From eq 13, the population of a conformer defined by an interval ΔQ with limiting values of the m conformational coordinates Q_1 and Q_2 is

$$p(\Delta Q) = [\int_{Q_1}^{Q_2} |G(Q)|^{-1/2} \exp[-V(Q)/kT] \prod_i^m dq_i]/z_{rv} \quad (14)$$

At this point, it is interesting to analyze the physical nature of the potential used in eq 13 in relation to the potentials used in previous molecular models.[7] We consider the potential at any one of the points, *a*, where the nonconformational coordinates are fully relaxed. For a molecule of N atoms and m conformational coordinates, expanding in Taylor series up to second order and considering the equilibrium condition respect to the nonconformational coordinates, we obtain

$$V_a = V_a^0 + \sum_i^m \left(\frac{\partial V}{\partial q_i}\right)_a \Delta q_i + \frac{1}{2}\sum_i^m \sum_j^m \left(\frac{\partial^2 V}{\partial q_i\, \partial q_j}\right)_a \Delta q_i \Delta q_j + \sum_i^m \sum_{j=m+1}^{3N-6} \left(\frac{\partial^2 V}{\partial q_i\, \partial q_j}\right)_a \Delta q_i \Delta q_j + \frac{1}{2}\sum_{i=m+1}^{3N-6} \sum_{j=m+1}^{3N-6} \left(\frac{\partial^2 V}{\partial q_i\, \partial q_j}\right)_a \Delta q_i \Delta q_j \quad (15)$$

Equation 15 shows that, for a linear approach, the potential is exactly a function of the m conformational coordinates. The second, third, and fourth terms exhibit a direct dependence on the conformational coordinates. The fourth and fifth terms involve nonconformational internal coordinates. In particular, the fifth term represents the effect of the nonconformational force constants. In ref 7 the "flexible model" assumes these force constants to be independent of the conformational coordinates. Thus, they emerge from the integral sign. However, the force constants depend parametrically on the conformational coordinates. Therefore, they should be kept in the integral. By using a relaxed potential, as defined in this work, we are taking into account this effect.

Results

Validity of the Semiclassical Approach. Rotational energy levels are so close at ambient temperature that the semiclassical approach is a good approximation. On the other hand, for the usual value of vibrational frequencies (say, in the range 1000−3000 cm^{-1}), the separation between the energy levels is higher than the ambient kT factor (about 200 cm^{-1}). Thus, the semiclassical approach is not applicable. However, the frequencies associated with the conformational motions (large amplitude vibrations) are low-frequency vibrations. For instance, the separation between the two first vibrational energy levels is calculated to be 141.43 and 48.35 cm^{-1}, for the methyl rotation of acetaldehyde[9a] and the rotation of the keto groups in malonaldehyde,[9c] respectively. In addition, the higher the molecular moiety experiencing the conformational motion, the smaller the kinetic B term in the quantum mechanical Hamiltonian, eq 7, and the smaller the vibrational frequency. It seems that for usual bioactive compounds, where the conformational changes affect groups higher than methyl or keto groups, the semiclassical approach could be an acceptable approximation. This assumption needs quantification.

We can get some insight on this problem by using the harmonic oscillator model at physiological temperature, 37 °C (310.15 K). The quantum mechanical vibrational partition

function is given by[12]

$$z_v^Q = \exp[-h\nu_0/2kT]/(1 - \exp[-h\nu_0/kT]) \qquad (16)$$

where the origin of energies has been taken in the zero of energies. In turn, the semiclassical vibrational partition function obtained from eq 16 is given as $z_v^{SC} = (kT - h\nu_0/2)/h\nu_0$. The difference between z_v^Q and z_v^{SC} can be quantified by defining an error function, E, (in percent) as

$$E = 100(z_v^Q - z_v^{SC}/z_v^Q) \qquad (17)$$

Figure 1 shows the error, E, as a function of ν_0 at physiological temperature. Fundamental frequencies up to 200 cm^{-1} are considered. We observe a linear variation of the error in this range of frequencies. In particular, the error is smaller than 10% for $\nu_0 \leq 44$ cm^{-1}.

To compare with the previous results, it is necessary to determine the range of anharmonic frequencies involved in the conformational motion of bioactive compounds. Thus, we simulate periodic motions with several periodicities, using potentials of the form

$$V(\theta) = V_0 + V_0 \cos(n\theta) \qquad (18)$$

In eq 18, V_0 is half the barrier height, $V_0 = H/2$, and n is the periodicity. Periodicities of 1, 2, and 3 are considered. We consider small (1 kcal mol^{-1}), medium (5 kcal mol^{-1}), and large (10 kcal mol^{-1}) barriers. As kinetic terms, we consider values of 1.0, 0.5, and 0.1 cm^{-1} for the B term, eq 7. These B values correspond to molecular moieties involving several heavy atoms (compare with the constant B term of 8.918 cm^{-1} for the methyl group in acetaldehyde[9c] or the 2.856 cm^{-1} for the keto group in malonaldehyde[9e]). The vibrational Hamiltonian, eq 7, is solved variationally in the free rotor basis using the program NIVELON,[16] which implements the methodology developed and described in refs 8c−8e. For two-fold and three-fold periodicities, the system can be classified under G_2 and G_3 nonrigid groups, isomorphic to the C_2 and C_3 point groups, respectively. Thus, the following symmetry adapted basis functions were employed for each irreducible representation:

G_2 group

$$a: \cos(2n\,\theta), \sin(2n\,\theta)$$

$$b: \cos((2n \pm 1)\,\theta), \sin((2n \pm 1)\,\theta)$$

G_3 group

$$a: \cos(3n\,\theta), \sin(3n\,\theta)$$

$$e: \cos((3n \pm 1)\,\theta), \sin((3n \pm 1)\,\theta) \qquad (19)$$

with $n = 0, 1, 2, \ldots$ A total of 400 basis functions were used to determine the stack of vibrational energy levels. To compare with the harmonic oscillator model, the position of the first vibrational energy level, E_0, measured from the bottom of the potential well, is selected. We consider that this datum defines a "harmonic" frequency as $\nu_0 = 2E_0$. Table 1 collects the ν_0 results of the simulations for the different combinations of kinetic terms and potential functions.

Table 1 shows that ν_0, and then the error for the associated semiclassical partition function, increases with the periodicity of the motion, with the B term, and with the potential barrier. The higher ν_0 is found for $B = 1.0$ cm^{-1} and a barrier of 10 kcal mol^{-1} in the three-fold case. The error, eq 17, is 39.2%. On the other hand, the smallest ν_0, 5.9 cm^{-1}, appears in the nonperiodical case for $B = 0.1$ cm^{-1} and for a barrier of 1.0 kcal mol^{-1}. Here, the error amounts to 1.4%. However, the barriers for conformational variations are usually smaller that 10 kcal mol^{-1}. In addition, the B kinetic terms for motions involving several heavy atoms are smaller than 1.0 cm^{-1} (for instance, a maximum value of 0.27 cm^{-1} for nicotine). Also, the periodicity decreases with the complexity of the molecule. Thus, a realistic average case can be a barrier of 5 kcal mol^{-1}, for 2-fold or no periodicity, and a B term of 0.1 or 0.5 cm^{-1}. Table 1 shows that in these conditions and two-fold periodicity, ν_0, amounts to 26.0 and 58.1 cm^{-1}, respectively. Using eq 17, the respective errors, are 6.0% and 13.2%. In the nonperiodical case, the corresponding errors are 3.0% and 6.7%. Thus, an error of a 10% can be used as an upper reference value.

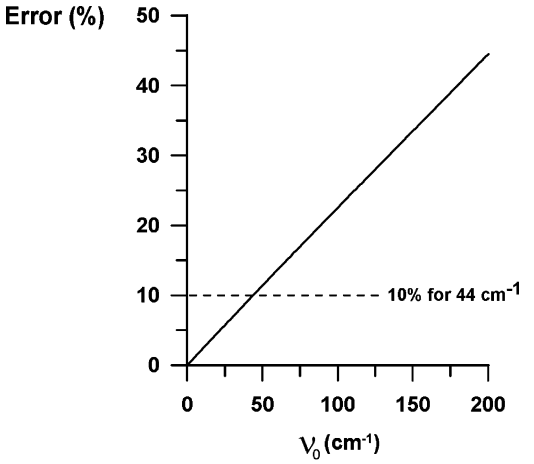

Figure 1. Error (in percent) between the quantum and semiclassical vibrational partition functions for the range of frequencies 1−200 cm^{-1}. Data at physiological temperature (37 °C).

TABLE 1: Fundamental Frequencies of Vibration Obtained as Twice the Energy, Measured from the Bottom of the Potential Well, of the First Vibrational Energy Level for Several Anharmonic Models[a]

B (cm^{-1})	H (kcal mol^{-1})	ν_0 (cm^{-1})[b]	ν_0 (cm^{-1})[c]	ν_0 (cm^{-1})[d]
1.0	1.0	18.6	36.9	55.0
0.5	1.0	13.2	26.2	39.1
0.1	1.0	5.9	11.8	17.6
1.0	5.0	41.7	82.0	124.4
0.5	5.0	29.5	58.1	88.2
0.1	5.0	13.2	26.0	39.6
1.0	10.0	59.0	117.8	176.4
0.5	10.0	41.8	83.4	124.9
0.1	10.0	18.7	37.4	56.0

[a] The table includes the kinetic term, B, and the height of the barrier, H, for the potentials considered. [b] No periodicity. [c] Two-fold periodicity. [d] Three-fold periodicity.

This value can be considered as an upper limit for the following reasons. First, when considering the stack of energy levels for a conformational motion, see refs 9c and 9e, a higher density of states is observed than is found for a harmonic motion Thus, the energy levels are closer than predicted by the harmonic model. This effect is translated in a higher number of states populated at a given temperature and, accordingly, in a smaller difference between the quantum and semiclassical partition functions. Second, when analyzing a conformational population distribution, we are using relative values arising from the same molecular model. Therefore, the error of the relative measure can be expected to be smaller than that of the individual data due to the cancellation of systematic errors. This same effect has been shown to reduce, in the worst case, almost by 50% the relative basis set superposition error in a set of several

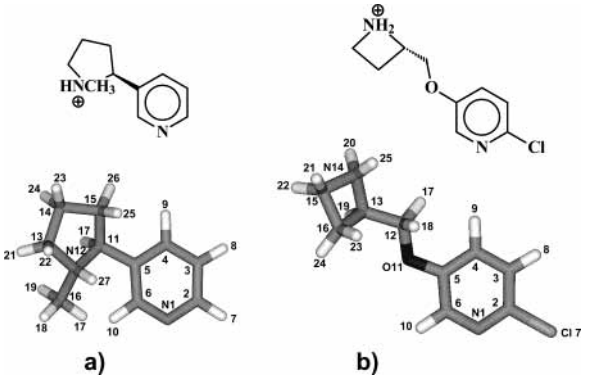

Figure 2. Structure and numbering convention of molecules considering in the work. (a) Protonated nicotine. (b) Protonated ABT-594. The heteroatoms are indicated in the numbering.

molecular complexes of aminopyridines.[17] Thus, we can conclude that for a typical flexible bioactive compound the semiclassical approach is able to reproduce the quantum results with an error smaller than 10%. In fact, the approach is better the larger the molecular moiety experiencing the variation.

Effect of the Conformational Kinetic Energy and the Rotovibrational Coupling. To determine the effect of these two factors we will consider the conformational population distribution of two molecules in a vacuum. First, the protonated nicotine will be considered, which is the bioactive form of the compound. This form exhibits only one conformational degree of freedom and medium potential energy barriers.[18] The second case corresponds to the nicotinic analgesic ABT-594 in its protonated, active, form. This is a two-dimensional case where two conformational coordinates can be defined. In addition, as shown previously,[19] the potential energy barriers are relatively high, about 40 kJ mol^{-1}.

Figure 2 shows the structure and numbering convention of nicotine and ABT-594 used in this work. The conformational coordinates are defined as θ(N12C11C5C4) for the protonated nicotine and θ_1(C13C12O11C5) and θ_2(N14C13C12O11) for the protonated ABT-594. In the structure used for nicotine, the *N*-methyl substituent is placed in trans with respect to the pyridine ring. Previous data[18] from molecular mechanics and from calculations at the MP2/6-31G(d, p)//HF/6-31G(d, p) and B3LYP/6-31G(d, p)//HF/6-31G(d, p) levels show that this is the minimum energy arrangement. The molecules are described at the MP2/cc-pVDZ level using the Gaussian 98 package.[20] A grid of points on each conformational coordinate is generated in increments of 30° for nicotine, and in increments of 60° for ABT-594.[19] At each point, the molecular structure is fully relaxed, keeping fixed the conformational coordinates. From the initial grid, the approximate placements of local minima are identified. The minima are obtained by fully relaxing the geometry from the closest point of the grid.

Figure 3 shows the potential energy variation for the two considered molecules. Figure 3a corresponds to the potential energy variation for protonated nicotine in a vacuum. Four minima, I to IV in increasing order of energy, are found. Minima I−III appear for values of the θ angle of 288.4°, 113.7°, and 218.9°, respectively. Minimum II appears at 0.3 kJ mol^{-1} of the global minimum. On the other hand, minimum III appears at 11.9 kJ mol^{-1}. The last minimum on θ, minimum IV, is located in the proximity of $\theta = 30°$. Full geometry relaxation from this geometry is unable to find the local minimum, leading instead to minimum II. However, the $\theta = 30°$ point is placed 15.9 kJ mol^{-1} from the global minimum. Thus, we can expect the population of this minimum to be negligible, as shown

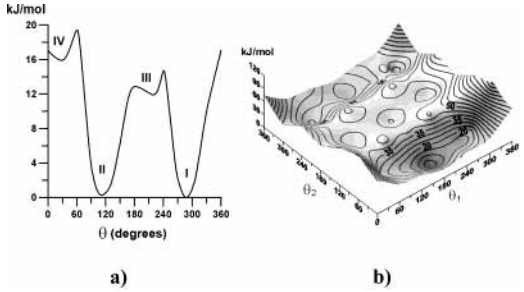

Figure 3. Potential energy maps. (a) Protonated nicotine. (b) Protonated ABT-594. Interval between isocontour lines 5 kJ mol^{-1}. All data are referred to the minimum value.

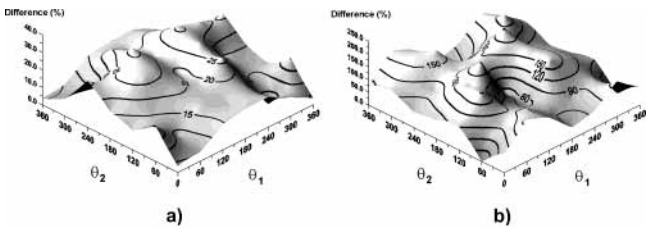

Figure 4. Variation, with the conformation, of the elements of the G matrix in the nicotinic analgesic ABT-594. (a) Variation of the pure rotational partition function. Interval between isocontour lines 5%. (b) Variation of the G matrix determinant. Interval between isocontour lines 30%. All data referred to the minimum value.

below. Therefore, the exact location of this minimum will not alter the population distribution of conformers. For this reason we keep the energy value for $\theta = 30°$ as the corresponding to minimum IV.

The close I and II minima correspond to conformations where the pyrrolidine and pyridinic rings are approximately perpendicular to each other. These data compare favorably with previous results for the trans form obtained by molecular mechanics, ab initio HF/6-31G(d, p) calculations,[18] and from fully relaxed MP2/6-31G(d, p) results.[21] This last work identifies two close minima, A and B (in order of energy) separated by less than 1.0 kcal mol^{-1}. These minima appear for a torsional angle, defined as (H17C11C5C6) using the numbering convention of Figure 2, close to 0° and 180°, respectively. These data can be compared favorably to the −7.2° and 178.6° values of the corresponding angle found for our conformers I and II.

Figure 3b shows the potential energy surface for the protonated ABT-594. The global minimum appears for $\theta_1 = 178.7°$, $\theta_2 = 43.8°$ (conformer VIII, following the nomenclature of ref 19), with some additional minima on the hypersurface that are extensively discussed elsewhere.[19] This minimum corresponds to a conformation where the additional proton on the azetidinyl group is oriented toward the electron lone pairs of the oxygen, O11. It has been determined that the same global minimum appears in aqueous solution.[19] The atoms in molecules (AIM) theory shows that this structure is stabilized by an intramolecular hydrogen bond between O11 and a hydrogen from one carbon on the azetidinyl group.[19] The minimum closest in energy appears at $\theta_1 = 271.2°$, $\theta_2 = 58.2°$, and is placed 11.6 kJ mol^{-1} above the global one. As it can be seen in Figure 3b, this second minimum almost merges with the first one. The remaining minima are placed higher in energy.

The failure of the usual assumption of a constant rotovibrational G matrix (in elements and determinant) is shown in Figure 4. Here, we use the two-dimensional case of ABT-594 to illustrate the dependence on the conformational coordinates of the rotational partition function (i.e., the individual elements of the G matrix giving rise to the inertial moments) and the G

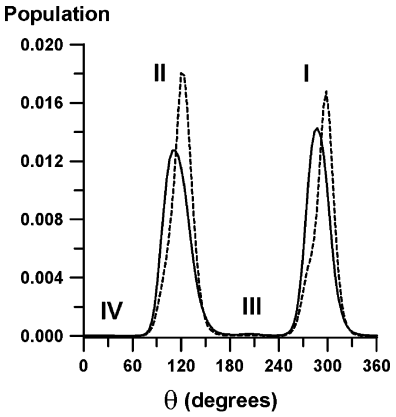

Figure 5. Conformational population for protonated nicotine. The dashed line corresponds to the population evaluated including the G matrix. The continuous line corresponds to the population evaluated using only the potential energy. Data at physiological temperature (37 °C).

matrix determinant. To obtain these data, the G matrix is computed for each grid point from the corresponding relaxed geometry. Figure 4a shows that the minimum value of the partition function is found for the conformation $\theta_1 = 300°$, $\theta_2 = 60°$. The maximum appears for $\theta_1 = 240°$, $\theta_2 = 180°$, with a difference representing a 28.4% of the minimum value. On the other hand, Figure 4b shows that the minimum value of the G matrix determinant appears at $\theta_1 = 0°$, $\theta_2 = 60°$. In this case the variation is very large. The difference with the minimum value reaches 215.7% for $\theta_1 = 240°$, $\theta_2 = 240°$. These results show that for a typical bioactive compound the elements of the rotovibrational G matrix cannot be considered constant with the conformation.

The next question is how, and how much, this variation of the G matrix affects the distribution of conformers. To such an end, eq 14 and eq 15 are applied to protonated nicotine and ABT-594 at physiological temperature, 37 °C. For each molecule, we have used the potential energy derived from the ab initio calculations. As previously, the G matrix determinant is computed for each grid point from the corresponding relaxed geometry. The integral in equations 14 and 15 is computed numerically using a set of bicubic splines in the two-dimensional case.[19,22,23] For the one-dimensional case, protonated nicotine, integration is carried out using the Rombert extrapolation, applying the trapezoidal rule.[23]

Figure 5 shows the population distribution of nicotine for two cases. In the first one (continuous line), we include only the potential energy, removing the effect of the G matrix determinant. In the second case (dashed line), we apply equations (14−15) without approximations. It is shown that only conformers I and II are significantly populated at physiological temperature. We observe that the inclusion of the G matrix changes the population distribution. Table 2 collects the population of conformers I to IV. The populations are computed integrating in the intervals determined by the minima arising in the population distribution. These minima correspond, approximately, to the intervals, 0°−60°, 60°−180°, 180°−230°, and 230°−360° for conformers IV, II, III, and I, respectively. Table 2 shows that the population of conformers III and IV at physiological temperature can be neglected. On the other hand, when only the potential energy is used, the population of conformers I and II are similar and very close to 50%. However, when the G matrix is included, the population of conformer I decreases, whereas it increases for conformer II. The result is

TABLE 2: Population (in percent) for the Conformers of Protonated Nicotine and ABT-594 When the G Matrix Is Considered[a]

	V	GV
conformer I nicotine	49.04	45.91
conformer II nicotine	50.37	53.76
conformer III nicotine	0.46	0.26
conformer IV nicotine	0.13	0.07
conformer VIII ABT-594	97.8	98.7

[a] Columns with V correspond to populations obtained using only the potential energy. Columns with GV indicate that the populations are computed using the potential energy and the G matrix determinant. Data at physiological temperature (37 °C).

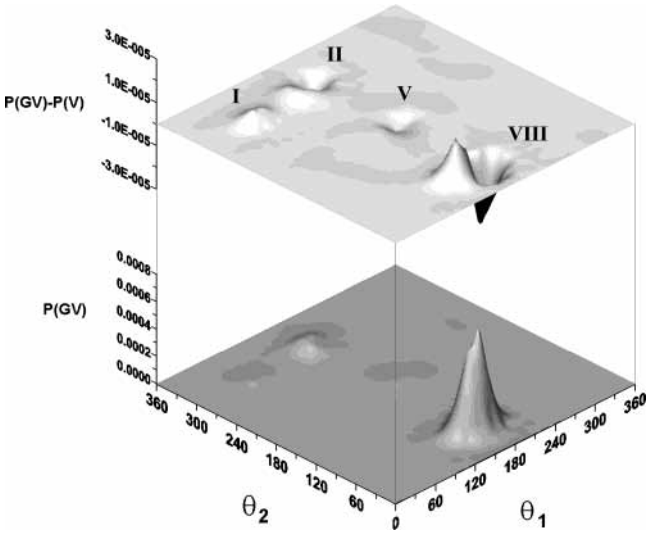

Figure 6. Conformational population for protonated ABT-594. The lower surface corresponds to the population evaluated including the G matrix. The upper surface corresponds to the difference between populations evaluated including and excluding the G matrix. Data at physiological temperature (37 °C).

that conformer II, the less energetically stable, is the most populated due to entropic effects.

Figure 6 collects the population distribution of ABT-594 as a function of θ_1 and θ_2. The population distribution, including the effects of the G matrix and the potential energy, is shown in the lower diagram. We observe that the conformer VIII (global minimum) is almost exclusively populated. The main difference of this case with respect to the protonated nicotine is the higher energy difference between the minima on the potential energy hypersurface, see Figure 3. In particular, no minimum is closer than 11.6 kJ mol^{-1} to the global minimum.

The results obtained by the exclusive use of the potential energy yields a distribution almost indistinguishable from the previous results. To display the difference between the two cases, we compute the difference between the map that includes both effects (G matrix and potential energy) and the map obtained from the potential energy. The result is shown in the upper part of Figure 6. We observe small differences for the minor conformers identified as I, II, and V, using again the nomenclature of ref 19. In particular, when we introduce the G matrix, conformer I is more populated, whereas conformers II and V decrease in population. On the other hand, for the most populated conformer, conformer VIII, the difference is positive and negative around the zone. However, all the differences are in the range -3.0×10^{-5} to 3.0×10^{-5}, which are low values (the base value in the population map shown in the lower part of Figure 6 is 10^{-6} to 10^{-7}). To quantify the effect of the inclusion of the G matrix in the population calculations, we

TABLE 3: Simulated Population (in %) of Conformers I and II of trans Nicotine, at Physiological Temperature (37 °C), as a Function of the Potential Energy Difference (ΔE) between Them[a]

	$\Delta E = 0.0$ kJ mol^{-1}		$\Delta E = 2.0$ kJ mol^{-1}		$\Delta E = 4.0$ kJ mol^{-1}		$\Delta E = 6.0$ kJ mol^{-1}		$\Delta E = 8.0$ kJ mol^{-1}		$\Delta E = 10.0$ kJ mol^{-1}	
	V	GV	V	GV	V	GV	V	GV	V	GV	V	GV
I	50.1	36.9	67.8	55.6	81.4	72.9	90.0	85.3	94.9	92.5	97.4	96.4
II	49.9	63.1	32.2	44.4	18.6	27.1	10.0	14.7	5.1	7.5	2.6	3.6

[a] Columns with V correspond to populations obtained using only the potential energy. Columns with GV indicate that the populations are computed using the potential energy and the G matrix determinant.

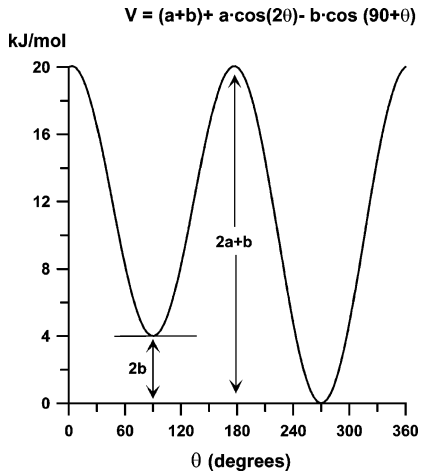

Figure 7. Model potential used to determine the effect of increasing energy differences between conformers.

compute the population of conformer VIII obtained including and excluding the G matrix. Since the base value of population in the population maps is 10^{-6} to 10^{-7}, we select as limits of integration for the peak the zone delimited by a population value of at least 10^{-6}. The results are collected in Table 2. We observe that including the G matrix, the population of conformer VIII changes only slightly from 97.8% to 98.7%.

The previous results show that the net effect of the G matrix depends on the difference in energy between the conformers. To quantify this effect, we compute the population variation for increasing energy differences between conformers. Thus, we simulate a one-dimensional potential with two minima, similar to the potential for nicotine shown in Figure 3a. The potential is defined as

$$V(\theta) = (a + b) + a\cos(2\theta) - b\cos(90 + \theta) \qquad (20)$$

This potential exhibits two minima at θ values of 90° and 270°. The minimum at 270° is the global one. The interconversion barrier is fixed at 20 kJ mol^{-1}. Figure 7 shows the physical meaning of the *a* and *b* parameters of eq 20. As G matrix values we have used the data obtained in the conformational analysis of nicotine. We have tested differences in energy between the conformers from 0.0 to 10.0 kJ mol^{-1} in increments of 2.0 kJ mol^{-1}. Table 3 shows the variation of population for increasing differences in energy between the conformers. In all cases, when the G matrix is included, conformer I decreases in population, whereas conformer II increases. Also, we observe that as ΔE increases the effect of the G matrix decreases. The absolute value of the population variation goes from 26.3% for $\Delta E = 0.0$ kJ mol^{-1} to 1.0% for $\Delta E = 10.0$ kJ mol^{-1}. In particular, the variation falls under 5% for $\Delta E = 8.0$ kJ mol^{-1} (about 2 kcal mol^{-1}). In fact, for this ΔE the variation reaches 2.5%. Thus, a difference of 2 kcal mol^{-1} between conformers can be taken as a practical limit for the potential energy to become the leading factor in the conformational population.

It is important to recall that the exclusive use of the potential energy is based on the assumption of the classical flexible model.[7] Thus, to be consistent with the model, the nonconformational coordinates should be fixed at some time-averaged values. Therefore, it is not physically consistent to compute the conformational partition function from a Boltzmann distribution involving only a relaxed potential. If a relaxed potential is used, eq 13 for the conformational partition function must be applied. Only when the difference between conformers is higher than about 2.0 kcal mol^{-1} can the effect of the G matrix be neglected.

Acknowledgment. This work has been supported by the "Junta de Comunidades de Castilla-La Mancha" (grant # PAI-02-001).

References and Notes

(1) Farnell, L.; Richards, W. R.; Ganellin, C. R. *J. Theor. Biol.* **1974**, *43*, 389−392.
(2) Richards, W. G. *Quantum Pharmacology*, 2nd ed.; Butterworths: London, 1983.
(3) Grant, G. H.; Richards, W. G. *Computational Chemistry* in *Oxford Chemistry Primers*; Oxford University Press: Oxford, 1995.
(4) Gõ, N.; Gõ, M.; Scheraga, H. A. *Proc. Nat. Acad. Sci. U.S.A.* **1968**, *59*, 1030−1037.
(5) Gõ, M.; Scheraga, H. A. *J. Chem. Phys.* **1969**, *51*, 4751−4767.
(6) Flory, P. J. *Macromolecules* **1974**, *7*, 381−392.
(7) Gõ, M.; Scheraga, H. A. *Macromolecules*. **1976**, *9*, 535−542.
(8) (a) Pickett, H. M. *J. Chem. Phys*. **1972**, *56*, 1715−1723. (b) Lewis, J. D.; Malloy, T. B., Jr.; Chao, T. H.; Laane, J. *J. Mol. Struct.* **1972**, *12*, 427−449. Harthcock, M. A.; Laane, J. *J. Phys. Chem*. **1985**, *89*, 4231−4240. (c) Muñoz-Caro, C.; Niño, A.; Moule, D. C. *Chem. Phys*. **1994**, *186*, 221−231. (d) Muñoz-Caro, C.; Niño, A. *Comput. Chem*. **1994**, *18*, 413−417. (e) Niño, A.; Muñoz-Caro, C. *Comput. Chem*. **1995**, *4*, 371−378.
(9) (a) Ozkabak, A. G.; Goodman, L. *J. Chem. Phys*. **1992**, *96*, 5958−5968. (b) Smeyers, Y. G.; Senent, M. L.; Botella, V.; Moule, D. C. *J. Chem. Phys*. **1993**, *98*, 2754−2767. (c) Niño, A.; Muñoz-Caro; C., Moule, D. C. *J. Phys. Chem*. **1994**, *98*, 1519−1524. (d) Niño, A.; Muñoz-Caro; C., Moule, D. C. *J. Phys. Chem*. **1995**, *99*, 8510−8515. (e) Niño, A.; Muñoz-Caro, C. *J. Phys. Chem. A* **1998**, *102*, 1177−1180.
(10) Niño, A.; Muñoz-Caro, C. *Comput. Chem*. **1994**, *18*, 27−32.
(11) Muñoz-Caro; Niño, A.; C., Moule, D. C. *J. Chem. Soc., Faraday Trans*. **1995**, *91*, 399−403.
(12) Lucas, K. *Applied Statistical Thermodynamics*; Springer-Verlag: Berlin, 1991.
(13) Wilson, E. B., Jr.; Decius, J. C.; Cross, C. *Molecular Vibrations*; Dover: New York, 1980. Re-publication of the original work of 1955 published by McGraw-Hill: New York.
(14) Podolsky, B. *Phys. Rev*. **1928**, *32*, 812−816.
(15) Goldstein, H. *Classical Mechanics*, 2nd ed.; Addison-Wesley: Reading, MA, 1980.
(16) Muñoz-Caro, C.; Niño, A. *QCPE Bull*. **1995**, *15*, 48.
(17) Muñoz-Caro, C.; Niño, A. *Biophys. Chem*. **2002**, *96*, 1−14.
(18) Elmore, D. E.; Dougherty, D. A. *J. Org. Chem*. **2000**, *65*, 742−747.
(19) Mora, M.; Muñoz-Caro, C.; Niño, A. *J. Comput.-Aided Mol. Des.*, in press.
(20) Frisch, M. J.; Trucks, G. W.; Schlegel, H. B.; Scuseria, G. E.; Robb, M. A.; Cheeseman, J. R.; Zakrzewski, V. G.; Montgomery, J. A., Jr.; Stratmann, R. E.; Burant, J. C.; Dapprich, S.; Millam, J. M.; Daniels, A. D.; Kudin, K. N.; Strain, M. C.; Farkas, O.; Tomasi, J.; Barone, V.; Cossi, M.; Cammi, R.; Mennucci, B.; Pomelli, C.; Adamo, C.; Clifford, S.; Ochterski, J.; Petersson, G. A.; Ayala, P. Y.; Cui, Q.; Morokuma, K.; Malick, D. K.; Rabuck, A. D.; Raghavachari, K.; Foresman, J. B.; Cioslowski, J.; Ortiz, J. V.; Stefanov, B. B.; Liu, G.; Liashenko, A.; Piskorz, P.; Komaromi, I.; Gomperts, R.; Martin, R. L.; Fox, D. J.; Keith, T.; Al-Laham, M. A.; Peng, C. Y.; Nanayakkara, A.; Gonzalez, C.; Challacombe, M.; Gill, P. M.

W.; Johnson, B. G.; Chen, W.; Wong, M. W.; Andres, J. L.; Head-Gordon, M.; Replogle, E. S.; Pople, J. A. *Gaussian 98*, revision A.7; Gaussian, Inc.: Pittsburgh, PA, 1998.

(21) Takeshima T.; Fukumoto R.; Egawa T.; Konaka S. *J. Phys. Chem. A* **2002**, *106*, 8734−8740.

(22) Engeln-Müllges, G.; Uhlig F. *Numerical Algorithms with Fortran*; Springer-Verlag: Berlin, 1996.

(23) Press, W. H.; Teukolsky, S. A.; Vetterling, W. T.; Flannery, B. P. *Numerical Recipes in Fortran 77*, 2nd ed.; Cambridge University Press: Cambridge, 1992.